CHAPTER 4

PREPARATION AND TRANSFERRIN CONJUGATION OF NANOPARTICLES

4. PREPARATION AND TRANSFERRIN CONJUGATION OF NANOPARTICLES

4.1 Introduction

There are a variety of nanoparticle systems currently being explored for cancer therapeutics (Haley et. al 2008). There is an increased interest in developing biodegradable nanoparticles since they offer a suitable means of delivering small molecular weight drugs, proteins or genes by either localized or targeted delivery to the tissue of interest (S.M. Moghimi et al 2001) The types of nanoparticles currently used in research for cancer therapeutic applications include dendrimers, liposomes, polymeric nanoparticles, micelles, protein nanoparticles, ceramic nanoparticles, viral nanoparticles, metallic nanoparticles, and carbon nanotubes. (J.D. Byrne et al., 2008). Amongst these nanoparticulate delivery systems polymeric nanoparticles have shown promising properties for targeted drug delivery and for sustained action. Nanoparticles are colloidal systems that range in size typically from 10 to 1000 nm in diameter, and are formulated from a biodegradable polymer in which the therapeutic agent is entrapped in, adsorbed or chemically coupled onto the polymer matrix (V. Labhasetwar 1997). Biodegradable polymers are unique tools for the preparation of nanoparticles, owing to their low toxicity profiles. [Si shen feng 2004] Despite the potential promise of cyanoacrylate polymers for brain targeting, the clinical safety of cyanoacrylates has not yet been established. Although a number of different polymers have been investigated for formulating biodegradable nanoparticles, polyepsilon caprolactone (PCL), poly (lactide-co-glycolide) (PLGA) and poly lactic acid (PLA), FDA approved biocompatible and biodegradable polymers, have been the most extensively studied (R. Langer 1997 and R.A. Jain 2000).

Nanoparticles can be prepared by polymerization of monomers entrapping the drug molecules leading to insitu polymerization or from preformed polymers. Several techniques have been suggested to prepare the biodegradable polymeric nanoparticles from preformed polymers such as poly (D, L-lactide) {PLA}, poly (D, L-glycolide) {PGA} and poly (D,L-lactide-co-glycolide) {PLGA}. Various methods proposed for the preparation of PLGA

nanoparticles include emulsification/solvent evaporation, solvent displacement/diffusion (nanoprecipitation), emulsification/solvent diffusion and salting out using synthetic polymers. Solvent diffusion (nanoprecipitation method) leads to the nanoparticles of uniform size and narrow size distribution. (Fessi et al., 1989) PVA is used as stabilizer to form particles of relatively small size and uniform size distribution (Sahoo et al, 2002 and P.D. Scholes et al 1993). As suggested by (Fessi et at. 1989, Chorny et al, 2002), addition of non-solvent, for PLGA, to the organic phase leads to the formation of smaller particle size. In the present study, we used ethanol as non-solvent (for PLGA) with the organic phase to achieve small particle size. Ethanol in the organic phase will reduce the solubility of PLGA in organic solvent which in turn will initiate early precipitation of the polymer upon contact with the aqueous phase and formation of a polymeric wall at a shorter distance from the primary nanodroplet centre, associated with a decrease in the size of NPs (Chorny et al., 2002).

Various formulation and process variables relating to effectiveness, safety, and usefulness should be optimized simultaneously when developing pharmaceutical formulations. The difficulties in optimizing a pharmaceutical formulation are due to the difficulty in understanding the real relationship between casual and individual pharmaceutical responses. A factorial design has often been applied to optimize the formulation variables (Misra A., Sheth A.K 2002; Levison KK et al, 1994; Shirakura O et al, 1991). The optimization procedure based on RSM includes statistical experimental designs, multiple regression analysis, and mathematical optimization algorithms for seeking the best formulation under a set of constrained equations. Since theoretical relationships between the response variables and causal factors are not clear, multiple regression analysis can be applied to the prediction of response variables on the basis of a second-order equation. In the present study, drug: polymer ratio, %w/v PVA concentration and volume of organic phase were selected as independent variables, whereas particle size and % EE were selected as dependent variables.

Surface modification of PLGA NPs has been attempted by either conjugating their surface with different ligands or conjugating ligands to the polymer followed by preparation of NPs. Ligands which have been reported are folic acid (Barbara Stella et al 2000), transferrin (Sanjeeb K. sahoo et al, 2004), biotin (T. Minko, 2004), lectins (Anjali sharma et al 2004) etc

These ligands bind specifically to the receptors on the plasma membrane of the target tissue which leads to the internalization of plasma membrane receptors along with the delivery system i.e. NPs.

PVA cross links with PLGA during the nanoparticle formation. The hydroxyl groups of PVA at the surface of nanoparticles are useful for the conjugation of ligand to the nanoparticle surface. The nanoparticles are first activated by reaction of epoxy group of polyglycidyl glycerol ether with the hydroxyl of PVA in the presence of zinc tetrafluoro borohydrate as catalyst. The activated nanoparticles are then reacted with ligand by linkage of the amino group of ligand with another epoxy of the polyglycidyl glycerol ether. The reaction of epoxy group is favoured at pH 5.0. (Sanjeeb K. sahoo et al, 2004)

Table 4.1 Materials and Equipments

Material	Source
Etoposide (ETP)	Gift sample from Cadila Pharmaceuticals, Ahmedabad, India
Temozolomide (TMZ)	Gift samples from V B Shilpa, Raichur, Karnataka, India.
Water (distilled)	Prepared in laboratory by distillation
PLGA (50:50)	Gift samples from Boehringer Ingelheim, Germany
Bichinconinic acid (BCA) protein Assay Kit	Banglore Genei, India
6-Coumarin	Gift sample from Neelikon dyes, Mumbai, India
Glacial acetic acid, potassium dihydrogen phosphate, disodium hydrogen phosphate, potassium chloride, potassium hydroxide, sodium chloride, sodium hydroxide, hydrochloric acid	S.D. Fine chemicals, Mumbai, India
HPLC grade methanol, acetonitrile acetic acid	S.D. Fine chemicals, India.
Nuclepore Polycarbonate membrane 2 µm 25mm	Whatman, USA
Polyvinyl alcohol	Sigma chemicals, USA
SR-4GL (hexa epoxy compound)	Gift sample from Sakamoto Yakuhin Kogyo Co., Ltd., Japan
Equipments	**Make**
Calibrated pipettes of 1.0 ml, 5.0 ml and 10.0 ml, volumetric flasks of 10 ml, 25 ml, 50 ml and 100 ml capacity, Funnels (i.d. 5.0 cm), beakers (250 ml) and other requisite glasswares	Schott & Corning (India) Ltd., Mumbai
Analytical balance	AX 120, EL 8300, Shimadzu Corp., Japan
pH meter	Pico^{+} Labindia, Mumbai, India
Cyclomixer, magnetic stirrer	Remi Scientific Equipments, Mumbai
Cooling Centrifuge	3K 30, Sigma Laboratory centrifuge, Osterode, GmBH.
Lyophilizer	DW1, 0-60E, Heto Drywinner, Denmark
UV-Visible Spectrophotometer	Shimadzu UV-1601, Japan
Spectrofluorimeter	Rf540, Shimadzu Corp., Japan
Particle and Zeta size Analyzer	Malvern zeta sizer NanoZS, U.K.
Transmission electron microscopy	Morgagni, Philips, Netherlands
^{1}H-NMR	av300, Bruker, UK
HPLC system	LC 20-AT prominence, Shimadzu Corp., Japan

4.2 Methods

4.2.1 Preparation and optimization of nanoparticles

The nanoparticles of both the drugs Etoposide (ETP) and Temozolomide (TMZ) were prepared suing the solvent diffusion (nanoprecipitation) technique [Fessi et. al, 1989]. The basic process parameters like rate of addition of organic phase and the speed of the magnetic stirrer were standardized before proceeding for the optimization of the formulation parameters. As known from the literature, the rate of addition of organic phase was kept at 0.5ml/min throughout the entire optimization process. The speed of the stirrer for further experiments was standardized using qualitative examination of nanoparticle dispersion. The process parameters were standardized using placebo batches without drug. The standardization of stirrer speed is tabulated in table 4.2

Table 4.2: Influence of Stirring Speed

Sr. No.	Stirrer speed	Observation
1	Low	Retention of solids at the surface of aqueous phase, resulting non uniform dispersion
2	Moderate	Uniform dispersion
3	High	Aggregation in the dispersion

ETP loaded PLGA nanoparticles [PLGA-ETP-NP] were prepared by nanoprecipitation technique shown in figure 4.1, as described by Fessi et al., 1989. On the basis of the preliminary experimentation critical formulation parameters were viz. drug: polymer ratio, % PVA concentration and organic: aqueous phase ratio. Briefly, 5mg ETP and PLGA (25mg, 50mg and 100mg corresponding to different drug: polymer ratio of 01:05, 01:10 and 01:20) were added to acetone: ethanol (90:10) mixture (at different volumes to make organic: aqueous phase ratio of 01:04, 01:03 and 01:02 equating to 0.25, 0.33 and 0.5 respectively in decimal values). The organic phase containing drug and polymer was injected at 0.5mL/min into vortex 10ml of aqueous phase containing PVA (0.5, 1 and 1.5%w/v) as stabilizer on a magnetic stirrer (Remi Equipments, Mumbai). With the diffusion of solvent in to the aqueous phase, the polymer precipitates while encapsulation of ETP also occur leading to formation PLGA-ETP-NP. The resulting nanoparticle dispersion was further stirred to

evaporate the organic phase. NPs were recovered by centrifugation for 30 min at 15000 rpm, washed thrice with distilled water to remove unentrapped drug and excess PVA.

TMZ loaded nanoparticles [PLGA-TMZ-NP] were prepared using the same procedure and parameters as with ETP nanoparticles with slight modification. The aqueous phase was adjusted to pH 4 with 0.1N HCl and to the organic phase was added 50µl of 0.1NHCl

Figure 4.1: Schematic representation of the nanoprecipitation process

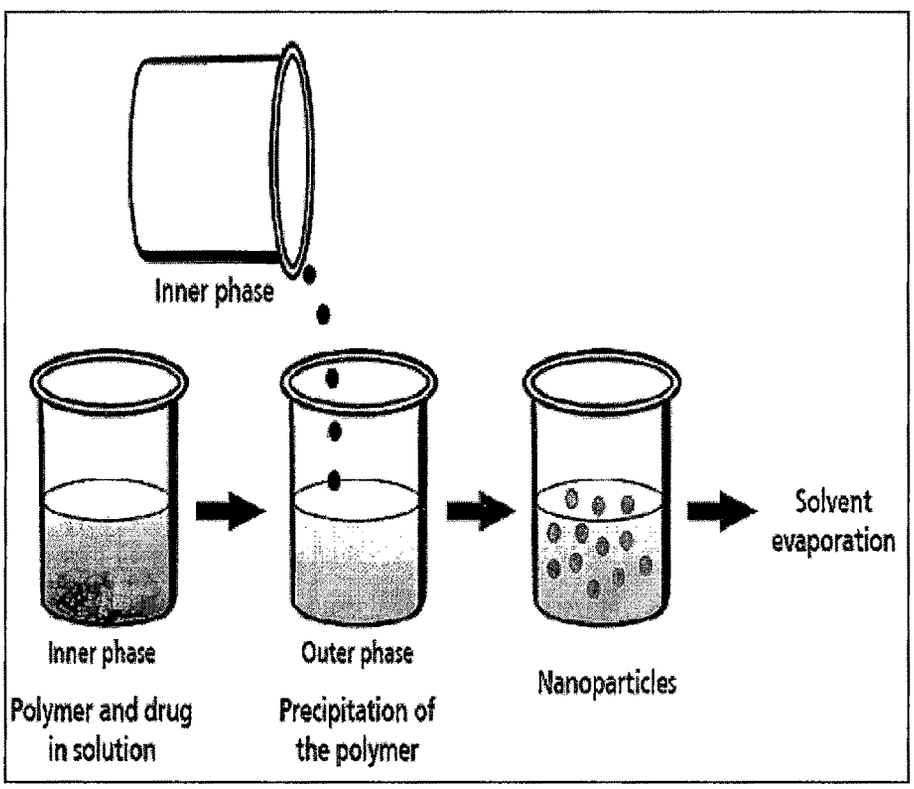

Optimization of formulation parameters

Pharmaceutical formulations are effected by single or combination of variables. It is difficult to assess the effect of the variables individually or in combination. Factorial designs allow all the factors to be varied simultaneously, thus enabling evaluation of the effects of each variable at each level and showing interrelationship among them. Factorial designs are of choice when simultaneous determination of the effects of several factors and their interactions on response parameters is required. A prior knowledge and understanding of the

process and the process variables under investigation are necessary for achieving a more realistic model. Initial experiments revealed the critical role of polymer concentration, stabilizer concentration and organic: aqueous phase ratio as major variables in determining the particle size and drug entrapment efficiency. Hence, polymer concentration, %w/v PVA concentration and organic: aqueous phase ratio were selected as independent variables to find the optimized condition for small particle size (PS) (<150nm) and higher % entrapment efficiency (%EE) using 3^3 factorial design and contour plots, whereas particle size and % EE were selected as response variables. The values of these selected variables along with their transformed values are shown in Table 4.3

Table 4.3: Coded values for the formulation parameters for preparation of nanoparticles

Coded Values	Independent Variables		
	Polymer conc. (mg). (X_1)	PVA conc. (%w/v) (X_2)	Org. Phase: Aq. Phase ratio (X_3)
-1	25	0.5	0.25
0	50	1	0.33
1	100	1.5	0.5

* The amount of the drug was fixed at 5mg and the polymer amount was changed

Twenty seven batches of nanoparticles were prepared by nanoprecipitation method according to the 3^3 experimental design shown in Table 4.4 for Etoposide and Table 4.5 Temozolomide. The prepared batches were evaluated for particle size, drug entrapment efficiency and the results were recorded in table 4.4 and table 4.5 for Etoposide and Temozolomide respectively.

Table 4.4: 3^3 factorial experimental design for PLGA-ETP-NP

Batch No.	X_1	X_2	X_3	PLGA-ETP-NP	
				PS (nm)	%EE
1	-1	-1	-1	153	54.7
2	0	-1	-1	168	63.1
3	1	-1	-1	173	65.9
4	-1	0	-1	164	57.6
5	0	0	-1	175	72.1
6	1	0	-1	182	76.9
7	-1	1	-1	168	64.5
8	0	1	-1	177	74.8
9	1	1	-1	186	79.2
10	-1	-1	0	135	49.6
11	0	-1	0	147	61.3
12	1	-1	0	152	64.1
13	-1	0	0	149	54.1
14	0	0	0	160	67.9
15	1	0	0	167	69.2
16	-1	1	0	156	57.3
17	0	1	0	169	69.2
18	1	1	0	178	70.2
19	-1	-1	1	116	43.7
20	0	-1	1	132	56.3
21	1	-1	1	143	59.1
22	-1	0	1	124	49.8
23	0	0	1	144	65.4
24	1	0	1	158	67.2
25	-1	1	1	128	52.3
26	0	1	1	152	66.1
27	1	1	1	164	68.3

Table 4.5: 3^3 factorial experimental design for PLGA-TMZ-NP

Batch No.	X_1	X_2	X_3	PLGA-TMZ-NP	
				PS (nm)	%EE
1	-1	-1	-1	139	24.6
2	0	-1	-1	156	31
3	1	-1	-1	169	32.7
4	-1	0	-1	156	31.6
5	0	0	-1	170	37.4
6	1	0	-1	176	42.2
7	-1	1	-1	159	34.4
8	0	1	-1	172	40.1
9	1	1	-1	181	45.9
10	-1	-1	0	131	22.4
11	0	-1	0	144	27.4
12	1	-1	0	155	30.9
13	-1	0	0	146	29.8
14	0	0	0	153	35.6
15	1	0	0	166	37.7
16	-1	1	0	152	34.5
17	0	1	0	164	37.9
18	1	1	0	172	40.2
19	-1	-1	1	107	14.5
20	0	-1	1	121	22.9
21	1	-1	1	142	26.1
22	-1	0	1	118	24.7
23	0	0	1	132	33.5
24	1	0	1	150	35.7
25	-1	1	1	136	27
26	0	1	1	145	34.2
27	1	1	1	154	38.7

Data Processing

A multilinear stepwise regression analysis was performed using Microsoft Excel software. Mathematical modeling was carried out by using Equation 1 to obtain a second-order polynomial equation.

$$Y = b_0 + b_1X_1 + b_2X_2 + b_3X_3\ b_{11}X_1^2 + b_{22}X_2^2 + b_{33}X3^2 + b_{12}X_1X_2 + b_13X_1X_3 + b_{23}X_2X_3 + b_{123}X_1X_2X_3 \quad \text{(Equation 1)}$$

Where b_0 is the arithmetic mean response of 27 runs and b_1, b_2 and b_3 is the estimated coefficients for the factors X_1, X_2 and X_3, respectively. The major responses represent the average result obtained by changing one factor at a time from its low to high value. The interactions show the change in particle size when two or more factors are varied simultaneously. The following equations were was derived by the best-fit method to describe the relationship of the particle size (Y_{PS}) and entrapment efficiency (Y_{EE}) with the polymer concentration (X_1), PVA concentration (X_2) and the ratio of org. phase: aq. phase (X_3). A full model was established after putting the values of regression coefficients in Equation 1.

Equations 2 and 3 represent the full model equations for PLGA-ETP-NP for particle size and entrapment efficiency respectively.

$$Y_{PS} = 160.5926 + 11.66667X_1 + 8.611111X_2 - 16.0556X_3 - 2.44444X_1^2 - 2.94444X_2^2 - 1.27778X_3^2 + 1X_1X_2 + 3.416667\ X_1X_3 + 1X_2X_3 + 1.375X_1X_2X_3 \quad \text{(Equation 2)}$$

$$Y_{EE} = 67.33704 + 7.583333X_1 + 4.672222X_2 - 4.47778X_3 - 4.92778X_1^2 - 2.26111X_2^2 + 0.622222X_3^2 + 0.2083333X_1X_2 + 0.3\ X_1X_3 - 0.61X_2X_3 - 0.3625X_1X_2X_3 \quad \text{(Equation 3)}$$

Equation 4 and 5 represent the full model equations for PLGA-TMZ-NP for particle size and entrapment efficiency respectively.

$$Y_{PS} = 155.1481 + 12.27778X_1 + 9.5X_2 - 15.1667X_3 - 0.27778X_1^2 - 1.94444X_2^2 - 4.61111X_3^2 - 2.41667X_1X_2 + 1.083333\ X_1X_3 + 1.416667X_2X_3 - 1.125X_1X_2X_3 \quad \text{(Equation 4)}$$

$$Y_{EE} = 35.8 + 4.811111X_1 + 5.577778X_2 - 3.47778X_3 - 1.46667X_1^2 - 2.83333X_2^2 - 0.86667X_3^2 + 0.058333X_1X_2 + 0.341667X_1X_3 + 0.358333X_2X_3 - 0.4125X_1X_2X_3 \quad \text{(Equation 5)}$$

Neglecting nonsignificant ($P > 0.05$) terms from the full model, a reduced model was established, which facilitates the optimization technique by plotting contour plots keeping

one major contributing independent formulation variable constant and varying other two independent formulation variables to establish the relationship between independent and dependent variables.

Equations 6 and 7 represent the reduced model equations for PLGA-ETP-NP for particle size and entrapment efficiency respectively.

$Y_{PS} = 158.2222 + 11.66667X_1 + 8.833333X_2 - 15.83333X_3 - 2.88889X_1^2 + 3.416667\ X_1X_3$ (Equation 6)

$Y_{EE} = 67.75185 + 7.583333X_1 + 4.672222X_2 - 4.47778X_3 - 4.92778X_1^2 - 2.26111X_2^2$ (Equation 7)

Equation 8 and 9 represent the reduced model equations for PLGA-TMZ-NP for particle size and entrapment efficiency respectively.

$Y_{PS} = 153.667 + 12.27778X_1 + 9.5X_2 - 15.1667X_3 - 4.61111X_3^2 - 2.41667X_1X_2$ (Equation 8)

$Y_{EE} = 35.2222 + 4.811111X_1 + 5.577778X_2 - 3.47778X_3 - 1.46667X_1^2 - 2.83333X_2^2$ (Equation 9)

ANOVA

Analysis of variance (ANOVA) of full model and reduced model was carried out and the F statistic was applied to check whether the nonsignificant terms can be omitted or not, from the full model. tables 4.6 to 4.7 show results of analysis of variance of full and reduced model for PS and %EE of etoposide nanoparticles and tables 4.8 to 4.9 show the results for temozolomide nanoparticles.

Table: 4.6 Analysis of Variance of Full and Reduced Model for PLGA-ETP-NP (PS)

		Df	SS	MS	F	R	R^2	Adj R^2
Regression	FM	10	8701.653	870.1653	105.671	0.992514	0.985085	0.975762
	RM	5	8557.157	1711.431	158.6952	0.987024	0.974217	0.968078
Error	FM	16	131.7546 (E1)	8.234664				
	RM	21	226.4722 (E2)	10.78439				

DF indicates Degree of freedom; E1 and E2 indicated Sum of squares of error of full and reduced model respectively; F, Fischer ratio; FM, full model; MS, Mean squares; RM, reduced model; and SS, Sum of squares.
Number of parameters omitted = 5.
†SSE2 – SSE1 = 226.4722-131.7546= 94.7176
‡MS of error (full model) = 8.234664
§F calculated = (94.7176/5)/ 8.234664= 2.30 ; F tabulated = 2.85
Since F cal < F tab, the omitted parameters are non significant and the hypothesis is accepted

Table 4.7: Analysis of Variance of Full and Reduced Model PLGA-ETP-NP (%EE)

		Df	SS	MS	F	R	R^2	Adj R^2
Regression	FM	10	1974.637	197.4637	74.78151	0.989471	0.979053	0.96596
	RM	5	1965.341	393.0683	160.1444	0.987139	0.974444	0.968359
Error	FM	16	42.24866 (E1)	2.640541				
	RM	21	51.5437 (E2)	2.454462				

Number of parameters omitted = 5.
†SSE2 – SSE1 = 51.5437-42.24866= 9.29504
‡MS of error (full model) = 2.640541
§F calculated = (9.29504 /5)/ 2.640541= 0.704025 ; F tabulated = 2.85
Since F cal < F tab, the omitted parameter is non significant and the hypothesis is accepted

Table 4.8: Analysis of Variance of Full and Reduced Model PLGA-TMZ-NP (PS)

		Df	SS	MS	F	R	R^2	Adj R^2
Regression	FM	10	8747.486	874.748	111.938	0.9929	0.9859	0.9771
	RM	5	8676.046	1735.209	185.468	0.9888	0.9778	0.9725
Error	FM	16	125.032 (E1)	7.814				
	RM	21	196.472 (E2)	9.355				

Number of parameters omitted = 5.
†SSE2 – SSE1 = 196.472 - 125.032 = 71.44
‡MS of error (full model) = 7.814
§F calculated = (71.44 /5)/ 7.814=1.8285; F tabulated = 2.85
Since F cal < F tab, the omitted parameter is non significant and the hypothesis is accepted

Table 4.9: Analysis of Variance of Full and Reduced Model PLGA-TMZ-NP (%EE)

		Df	SS	MS	F	R	R^2	Adj R^2
Regression	FM	10	1264.284	126.4284	73.71133	0.98932	0.978755	0.965477
	RM	5	1255.433	251.0867	145.2834	0.985852	0.971903	0.965214
Error	FM	16	27.44292 (E1)	1.715182				
	RM	21	36.29333 (E2)	1.728254				

Number of parameters omitted = 5.
†SSE2 – SSE1 = 36.29333-27.44292= 8.85041
‡MS of error (full model) = 1.715182
§F calculated = (8.85041/5)/ 1.715182=1.032; F tabulated = 2.85
Since F cal < F tab, the omitted parameter is non significant and the hypothesis is accepted

Construction of contours:

Two dimensional contour plots were established using the reduced polynomial equations. At fixed levels of -1, 0 and 1 of independent variable with highest coefficient value, values of independent variables were computed for particle size and entrapment efficiency and contour plots were established The contours for etoposide and temozolomide are shown in Fig. 4.2 to 4.3and Fig. 4.4 to 4.5 respectively

Figure 4.2: Contour plot for particle size of PLGA-ETP-NP

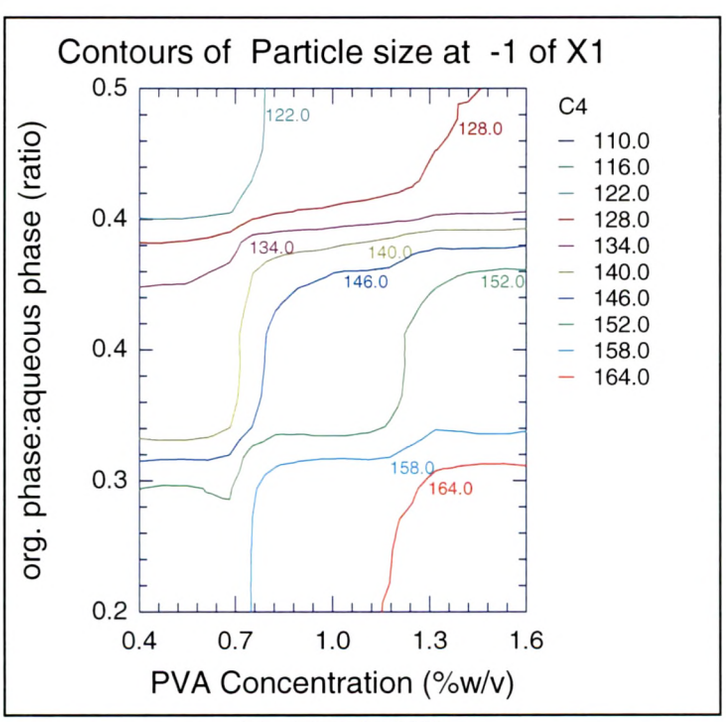

(a) -1 level of X1

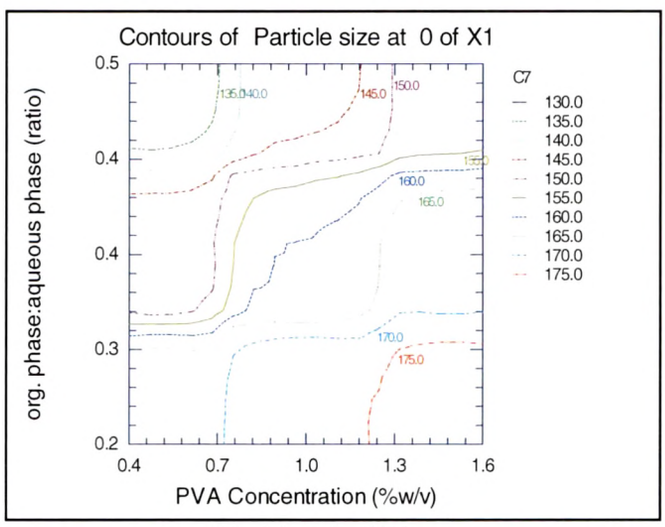

(b) 0 level of X1

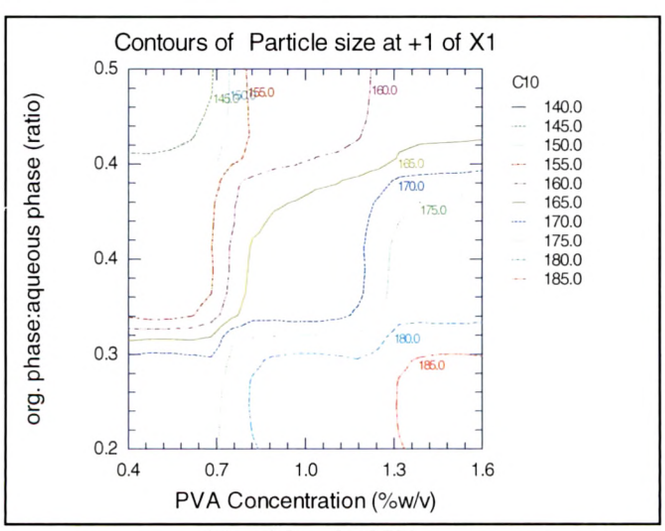

(c) +1 level of X1

Figure 4.3: Contour plot for drug entrapment efficiency of PLGA-ETP-NP

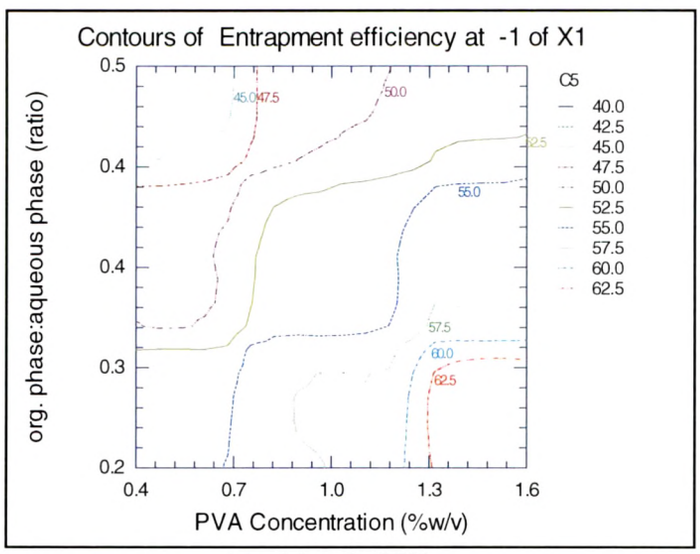

(a) -1 level of X1

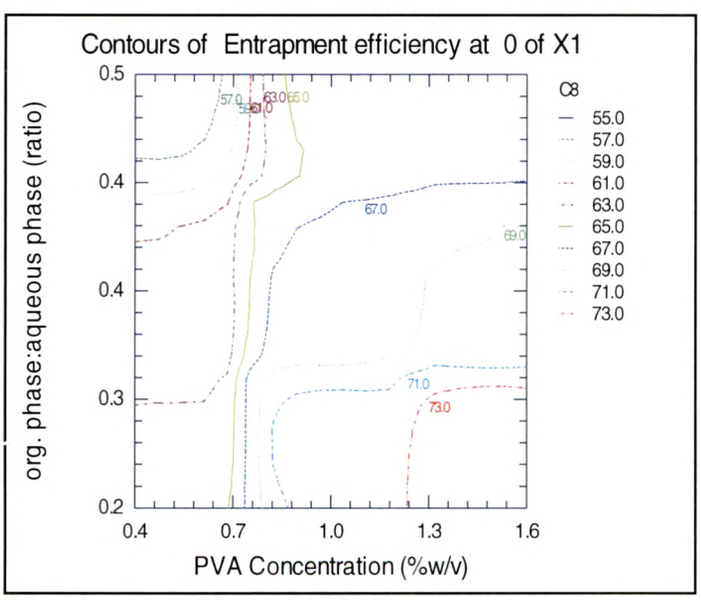

(b) 0 level of X1

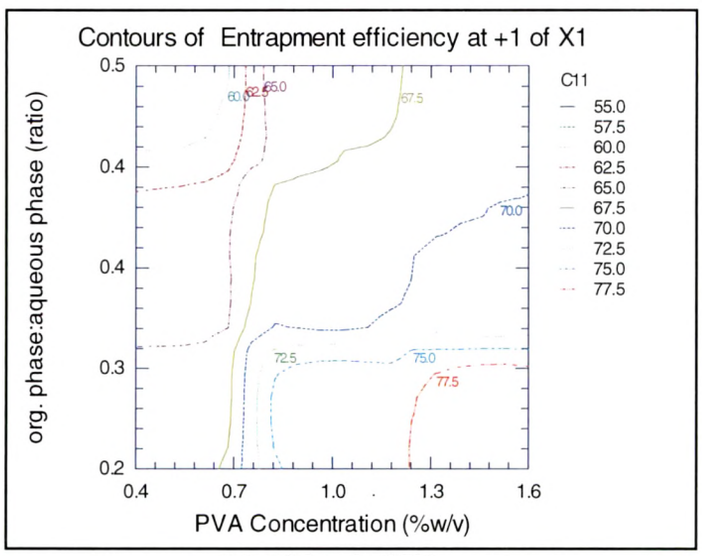

(c) +1 level of X1

Figure 4.4: Contour plot for particle size of PLGA-TMZ-NP

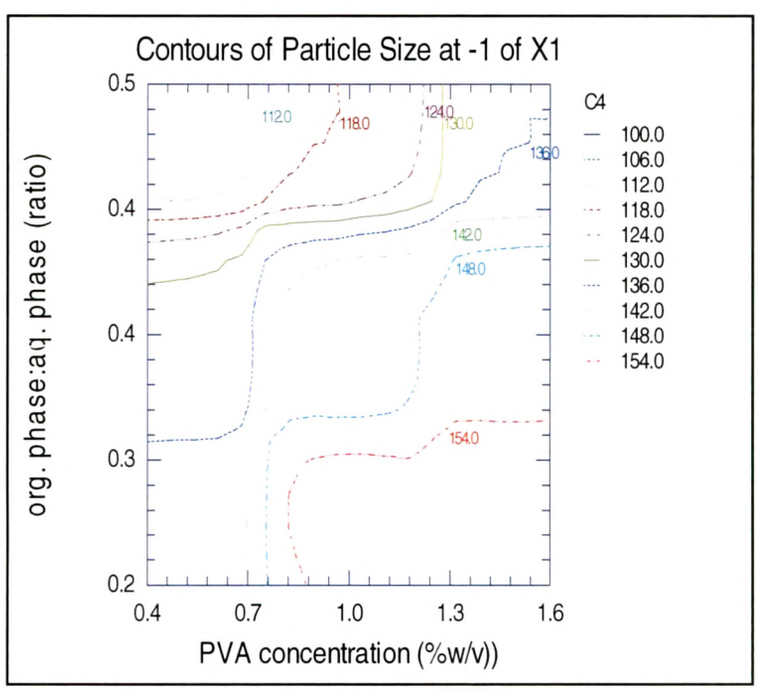

(a) -1 level of X1

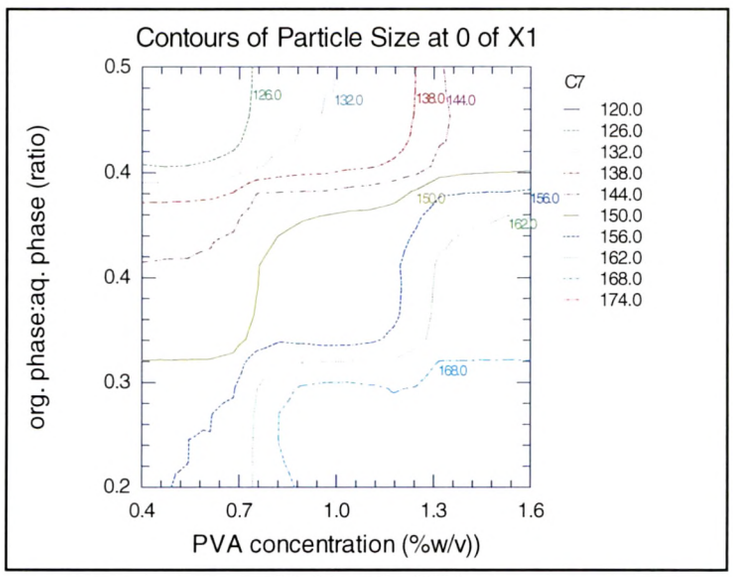

(b) 0 level of X1

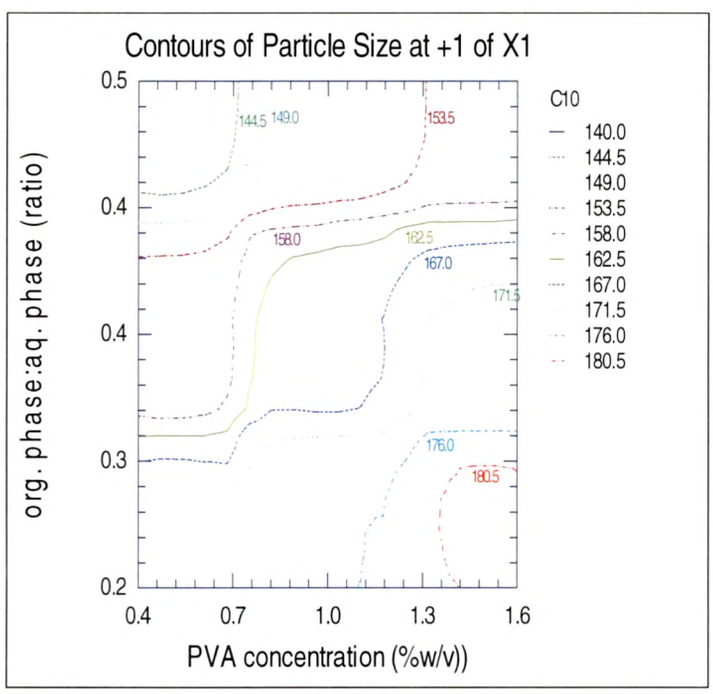

(c) +1 level of X1

Figure 4.5: Contour plot for drug entrapment efficiency of PLGA-TMZ-NP

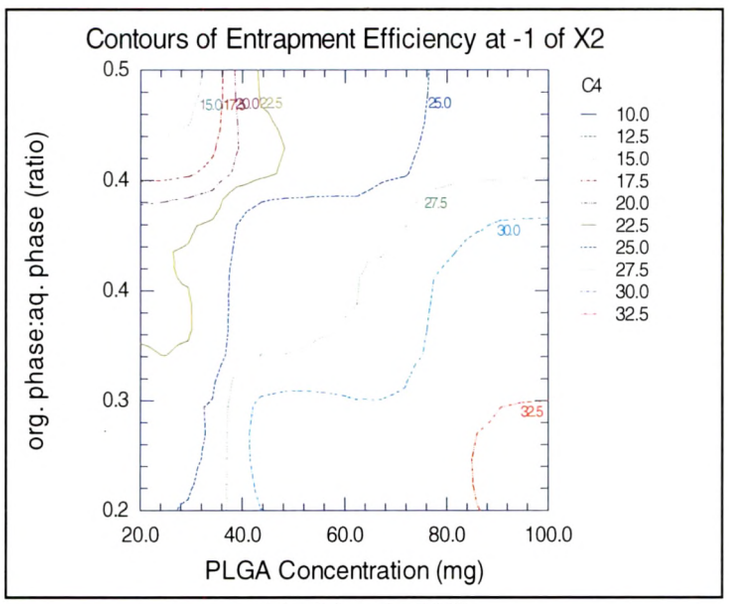

(a) -1 level of X2

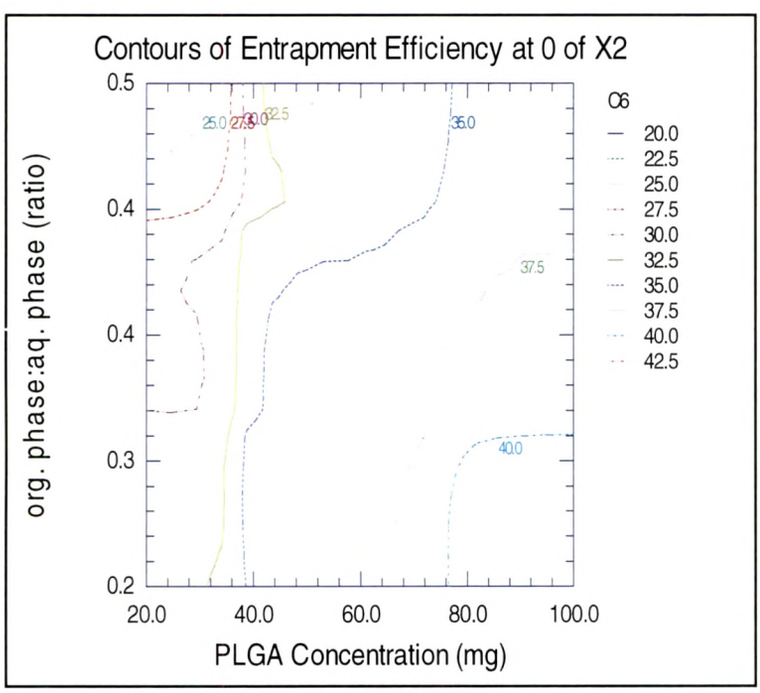

(b) 0 level of X2

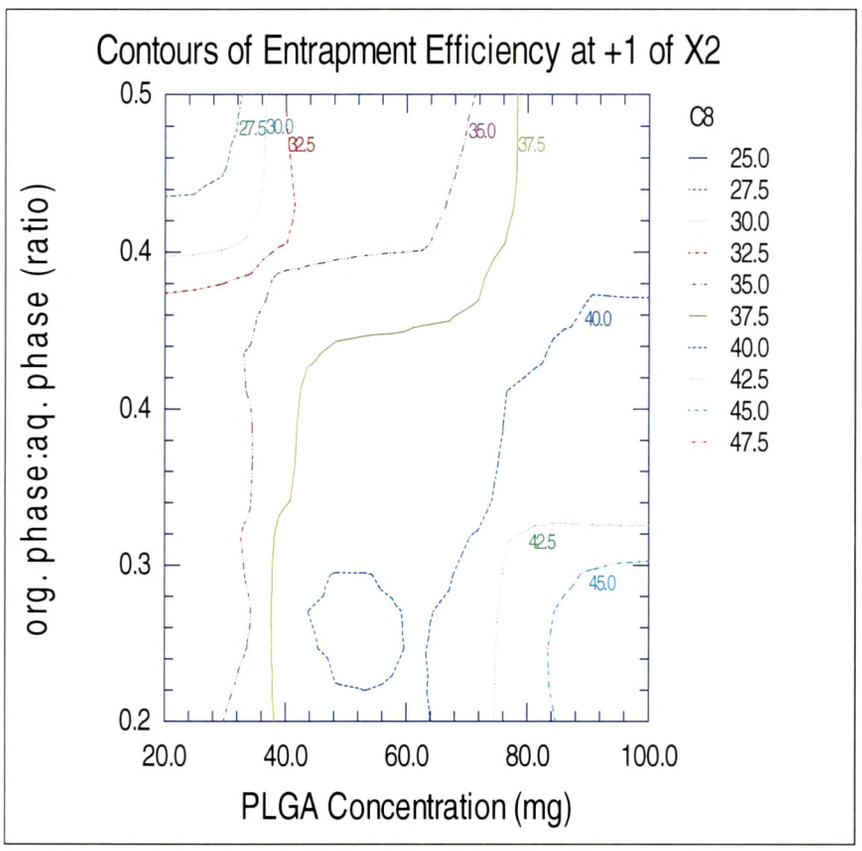

(c) +1 level of X2

Check Point Analysis

A check point analysis was performed to confirm the utility of established contour plots and reduced polynomial equation in the preparation of etoposide and temozolomide nanoparticles. Values of two independent variables were taken from three check points each on contour plots plotted at fixed levels i.e -1, 0 and 1 of independent variable of highest coefficient and the values of particle size and entrapment efficiency were generated by NCSS software. Nanoparticles were prepared experimentally by taking the amounts of the independent variables on the same check points. Each batch was prepared in triplicate and mean values were determined and tabulated in Table 4.10 for etoposide and in Table 4.11, 4.12 for temozolomide. Difference of theoretically computed values of particle size and entrapment efficiency and the mean values of experimentally obtained particle size and entrapment efficiency were compared by using student't' test method.

Table 4.10: Check point analysis for PLGA-ETP-NP

No.		Values from contours		Particle Size (nm)		% Entrapment Efficiency	
	X_1	X_2	X_3	Predicted	Experimental	Predicted	Experimental
1	-1	0.75	0.29	155.6	156.8 ±4.03	55.53	54.23±1.76
2	0	1.18	0.34	161.3	159.8±2.71	68.16	69.43±2.14
3	1	1.38	0.41	171.4	170.7±1.18	69.36	67.89±1.36
		P-value		0.7176		0.6295	

Table 4.11: Check point analysis for particle size for PLGA-TMZ-NP

No.		Values from contours		Particle Size (nm)	
	X_1	X_2	X_3	Predicted	Experimental
1	-1	0.75	0.29	147.2	148.9 ±2.94
2	0	1.18	0.34	154.5	152.2±1.78
3	1	1.38	0.41	164.4	168.4±2.17
		P-value		0.6008	

Table 4.12: Check point analysis for entrapment efficiency for PLGA-TMZ-NP

No.		Values from contours		% Entrapment Efficiency	
	X_2	X_1	X_3	Predicted	Experimental
1	-1	43.53	0.29	29.15	32.98 ± 1.83
2	0	71.76	0.34	36.31	34.22 ±0.68
3	1	85.88	0.41	39.40	43.17 ± 0.89
		P-value		0.4483	

4.2.2 Lyophilization and optimization of cryoprotectant concentration

The nanoparticle dispersions have thermodynamic instability upon storage and lead to the formation of aggregates. Freeze drying/lyophilization is one of the known methods to recover the nanoparticles in the dried form and suitably redisperse it at the time of administration. To the suspension of the nanoparticles different cryoprotectants like sucrose, mannitol and trehalose were added in different concentrations at nanoparticle (NP): cryoprotectant (CP) ratio of 1:1, 1:2 and 1:3 before freeze-drying. The effect these cryoprotectants on the redispersibility of the freeze-dried formulations and the size of the nanoparticles after freeze-drying was investigated and recorded in table 4.13

4.2.3 Transferrin conjugation of nanoparticles

Transferrin (Tf) was conjugated to the surface of the PLGA nanoparticles by using a two step process as described by (Sahoo et al, 2004). Transferrin was conjugated to the hydroxyl group of surface cross linked PVA. In the first step, the nanoparticles were activated using an epoxy compound and in the second step, the activated nanoparticles were conjugated to transferrin.

Figure 4.6: Schematic diagram of conjugation of transferrin to nanoparticle surface

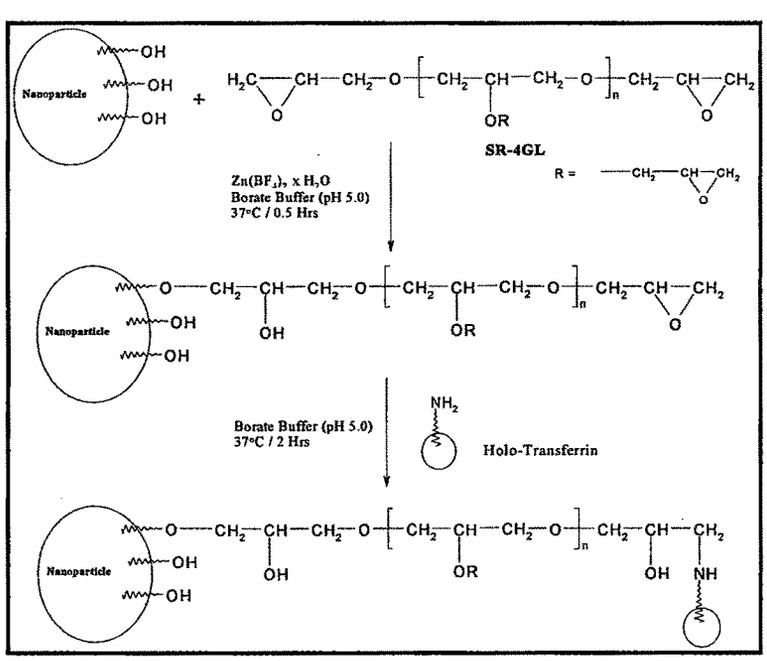

Briefly to the lyophilized NPs (4mg/ml) dispersed in borate buffer (5ml, pH 5.0 50mM), was added zinc tetrafluoroborate hydrate as a catalyst and a solution of SR-4GL (epoxy compound that acts as a linker) in borate buffer. The reaction mixture was stirred on a magnetic stirrer at 37°C for 30mins. The NPs were centrifuged at 15,000 rpm for 30mins at 4°C and were washed thrice with borate buffer to remove unreacted SR-4GL. In the second step, to the dispersion of the epoxy-activated NPs (4mg/ml) was added a solution of Tf in borate buffer and the reaction mixture was stirred for on magnetic stirrer at 37°C for 2hrs. The NPs were centrifuged at 15,000 rpm for 30mins at 4°C, to remove the unreacted transferrin. The NPs were washed twice with borate buffer and were lyophilized for 24hrs.

Influence of amount of activating agent [Epoxy compound: SR-4GL]

The influence of the amount of activating agent (SR-4GL) on the surface Tf density and particle size was checked by varying the amount of SR-4GL, keeping the weight of nanoparticles (20mg), catalyst (5mg) and the amount of Tf taken for conjugation (10mg) constant. The results for both Etoposide and Temozolomide nanoparticles are recorded in table 4.14 and graphically are represented in fig 4.7 & 4.8 for etoposide nanoparticles and fig 4.9 & 4.10 for temozolomide nanoparticles.

Influence of amount of Transferrin (Tf)

Influence of amount of Tf (taken for conjugation) on surface Tf density and particle size was checked by varying the amount of Tf added 20 mg of activated nanoparticles. The results for both Etoposide and Temozolomide are recorded in table 4.15 and graphically represented in fig 4.11 & 4.12 for etoposide nanoparticles and fig 4.13 & 4.14 for temozolomide nanoparticles.

Estimation of surface Transferrin density

To estimate the amount of transferrin conjugated to the surface of nanoparticles, the amount of transferrin in the supernatant and the washings was subtracted from the amount of transferrin taken for conjugation. The amount of transferrin conjugated to the surface of the nanoparticles was calculated using the following expression

Surface density of Tf = (Amount of the Tf conjugated/weight of the nanoparticles taken for conjugation)

^{1}H]NMR of the Tf conjugated nanoparticles

^{1}H-NMR spectroscopy was used to ascertain the conjugation of Tf to the nanoparticles. The ^{1}H-NMR spectra of Tf-PLGA-ETP-NP and Tf-PLGA-TMZ-NP are shown in Fig.4.15 and Fig. 4.16 respectively.

4.2.4 Preparation of 6-coumarin loaded nanoparticles

Nanoparticles containing fluorescent containing dye 6-coumarin were formulated using the nanoprecipitation method. The dye acts as a fluorescent probe for NPs and offers a sensitive method to quantitatively determine their intracellular uptake (Panyam et al., 2003). Briefly, 50μg of the dye and 50mg of PLGA were dissolved in organic phase (acetone: ethanol-90:10) and added dropwise at 0.5ml/min to vortex of the 1%w/v aqueous solution of PVA kept on stirring. After evaporation of the solvent, NPs were recovered by centrifugation for 30 min at 15000 rpm, washed three times with distilled water to remove unentrapped dye and excess PVA, and then lyophilized for 24 hrs (Heto Drywinner, Denmark). The nanoparticles were further conjugated with Tf, using the parameters conditions optimized for drug loaded nanoparticles. Results of characterization of 6-coumarin nanoparticles are tabulated and discussed in chapter 5.

4.3 Results and Discussion

The nanoprecipitation method developed by Fessi et al., represents an easy and reproducible technique and very often used to prepare nanoparticles from PLGA polymer. The method followed is represented hereby in a flow chart

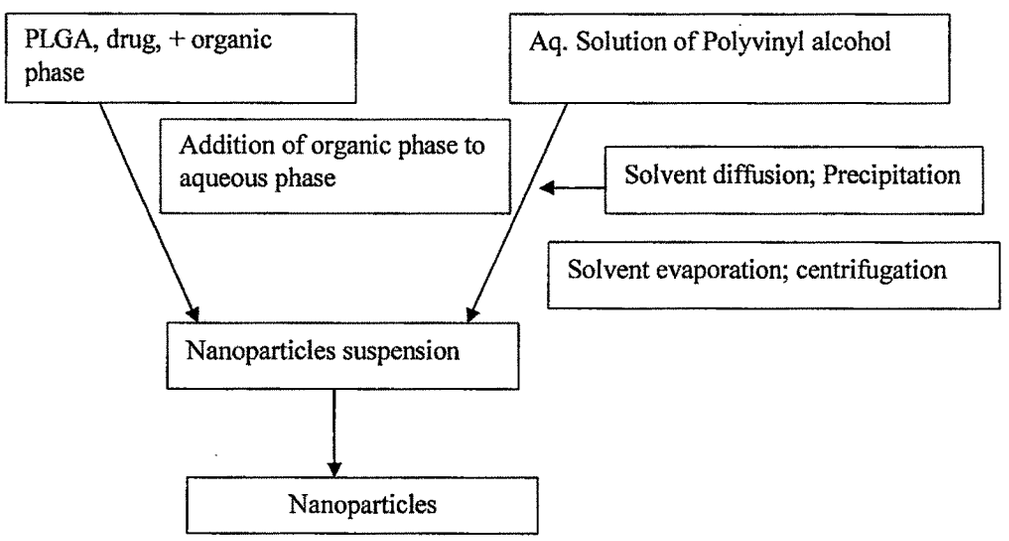

4.3.1 Preparation and optimization of nanoparticles

The process parameters such as the stirrer speed and rate of addition of organic phase affect the formation of the nanoparticles. As commonly reported in the literature (Fessi et al. 1989, Derakhshandeh et al., 2007) the rate of addition of the organic phase to the aqueous phase was kept constant at 0.5ml/min. The speed of stirring was evaluated for the formation of nanoparticles. The process was executed at slow, moderate and high speed of the stirrer and the observations are tabulated in table 4.2. At moderate speed of the stirrer there was uniform nanoparticle dispersion with no particle aggregation. However, at slow speed the vortex formation was inadequate and hence leads to the deposition of the solids at the surface of the aqueous phase. At high stirrer speed there was aggregation of the nanoparticles. This may be due to the high shear causing insufficient stabilization of nanoparticles and causing particle

aggregation. Hence the all the batches further were prepared at the moderate speed of the stirrer.

Optimization of formulation parameters

In this study, the main parameters affecting the nanoparticle formulation were found to be polymer concentration (keeping the amount of the drug constant), %w/v PVA concentration in aqueous phase and the ratio of the organic: aqueous phase (represented in decimal form). Hence, polymer concentration, %w/v PVA concentration and organic: aqueous phase ratio were selected as independent variables to find the optimized condition for small particle size (PS) (<150nm) and highest % drug entrapment efficiency (%EE) using 3^3 factorial design and the results are recorded in table 4.4 for Etoposide and table 4.5 for Temozolomide.

For intravenous administration, particle size < 200nm is preferred to prevent opsonization. In this study, the drug loaded PLGA nanoparticles were to be surface conjugated with ligand further. Hence the optimization criteria for particle size of drug loaded nanoparticles was kept as < 150nm with highest drug entrapment efficiency

Influence of the Polymer (PLGA) Concentration

For both Etoposide and Temozolomide nanoparticles, the increase in the concentration of PLGA resulted in the increase in the particle size of the nanoparticles. The viscosity of the organic phase in which the PLGA is dissolved appears to affecting the nanoparticles size due to hindrance in rapid dispersion of PLGA solution into the aqueous phase and resulted increase in the droplet and nanoparticle size. (Chorny et al., 2002) Availability of PVA on the surface of nanoparticles prevents the aggregation of nanoparticles during solvent evaporation but due to higher PLGA concentration, deposition of PVA on the particle surface may not be uniform and sufficient leading to aggregation. Increase in concentration of PLGA increases the drug entrapment efficiency for both Etoposide and temozolomide. It may be due to increase in drug entrapping polymer and due to the decrease in the diffusion of the drug towards the aqueous phase. (Song et al 2008 a, b).

Influence of PVA concentration

The increase in the PVA concentration leads to increase of particle size of nanoparticles. This increase in the nanoparticles size may be due to increase in the viscosity of the aqueous phase thereby increasing the resistance to the diffusion rate of the organic phase. The miscibility of organic phase (acetone) with aqueous phase results in orientation of PVA at the interface of PLGA solution in acetone present as droplets in the system (Sahoo et al., 2002). The increase in the PVA concentration leads to enhanced orientation of PVA towards PLGA and hence increases in the particle size. The drug entrapment efficiency was also found to increase with increase in the PVA concentration. This increase in the drug entrapment efficiency may be probably due to reduction in diffusion rate of the organic phase in the aqueous phase.

Influence of the organic: aqueous phase ratio

The particle size and drug entrapment efficiency were found to be inversely proportional to the organic: aqueous phase ratio. As the organic: aqueous phase ratio was increased, the particle size and drug entrapment efficiency decreased for etoposide and temozolomide. The increase in the organic phase ratio leads increased evaporation time causing slower polymer precipitation, due to the increased microenvironment provided by organic phase after dispersing in the aqueous phase, and thereby formation of small particles. Due to the increased evaporation time and slower polymer precipitation, the tendency of the drug to escape in the aqueous phase before polymer precipitation increases leading to lower drug entrapment efficiency.

Multiple regression analysis

Twenty-seven batches for each of etoposide and temozolomide nanoparticles were prepared by nanoprecipitation method using 3^3 factorial design (table 4.3) varying three independent variables namely polymer concentration(X_1), %w/v PVA concentration (X_2) & organic: aqueous phase ratio (X_3). The influence of these independent variables on the dependent variables particle size (PS) and % drug entrapment efficiency (%EE) was evaluated. The results for Etoposide nanoparticles are recorded in table 4.4 and for Temozolomide in table 4.5.

The PS and %EE obtained at various levels of three independent variables (X_1, X_2 and X_3) were subjected to multiple regression. Second order polynomial equations (full model) were obtained.

The effects of X_1, X_2 and X_3 on PS and % EE were evaluated by changing one variable at a time from its low to high value. The interactions (X_1X_2, X_1X_3, X_2X_3 and $X_1X_2X_3$) show how the particle size and entrapment efficiency changes when two or more variables were simultaneously changed.

For etoposide, the particle size and entrapment values for the 27 batches showed a wide variation starting from a minimum of 116nm to maximum of 186nm and minimum of 43.7% to maximum of 79.8% respectively as shown in table 4.4. The coefficients of terms X_2^2, X_3^2, X_1X_2 X_2X_3, and $X_1X_2X_3$ ($p>0.05$) in equation 2 are regarded as least contributing to the PS of etoposide. Similarly, the coefficients of terms X_3^2, X_1X_2, X_1X_3, X_2X_3 and $X_1X_2X_3$ (having $p>0.05$) in equation 3 are regarded as least contributing to the %EE of etoposide. Hence, these terms were neglected from full model considering non-significant and reduced polynomial equation 6 and equation 7 were obtained for PS and %EE by including significant terms ($p<0.05$) of equation 2 and equation 3 respectively.

F-statistic of the results of ANOVA of full model and reduced model (as represented in table 4.6 and table 4.7) confirmed omission of non-significant terms of equation 2 and equation 3. Since Fcal (2.30) < Ftab (2.85) for PS and Fcal (0.704) < Ftab (2.85) for %EE ($a = 0.05$, $v_1 = 5$ and $v_2 = 16$), it was concluded that the neglected terms do not significantly contributing in predicting of particle size and entrapment efficiency. When the coefficient values of three independent key variables (X_1, X_2, & X_3) in equation 6 and equation 7 were compared, the value for variable X_1 ($b_1 = 11.666$ for particle size, $b_1 = 7.583$ for entrapment efficiency) was found to be maximum and hence the variable X_1 was considered to be a major contributing variable for particle size and entrapment efficiency of PLGA-ETP-NP.

Similarly, for temozolomide the PS and %EE values for the 27 batches ranged from minimum of 107nm to maximum of 181nm and minimum of 14.5% to maximum of 45.9% respectively as shown in table 4.5. The low drug entrapment efficiencies for Temozolomide

were due to the hydrophilic nature of Temozolomide and hence partition into the aqueous phase. The coefficients of terms X_1^2, X_2^2, X_1X_3, X_2X_3 and $X_1X_2X_3$ ($p>0.05$) in equation 4 are regarded as least contributing to the particle size of temozolomide. Similarly, the coefficients of terms X_3^2, X_1X_2, X_1X_3, X_2X_3 and $X_1X_2X_3$ (having $p>0.05$) in equation 5 are regarded as least contributing to the entrapment efficiency of temozolomide. Hence, these terms were neglected from full model considering non-significant and reduced polynomial equation 8 and equation 9 were obtained for PS and %EE by including significant terms ($p<0.05$) of equation 4 and equation 5 respectively.

F-statistic of the results of ANOVA of full model and reduced model (as represented in table 4.8 and table 4.9) confirmed omission of non-significant terms of equation 4 and equation 5. Since Fcal (1.8285) < Ftab (2.85) for PS and Fcal (1.032) < Ftab (2.85) for EE ($a = 0.05$, $v_1 = 5$ and $v_2 = 16$), it was concluded that the neglected terms do not significantly contributing in predicting of particle size and entrapment efficiency. When the coefficient values of three independent key variables (X_1, X_2, & X_3) in equation 8 and equation 9 were compared, the value for variable X_1 ($b_1 = 12.27778$ for particle size) and the value of variable X_2 ($b_2 = 5.77778$ for entrapment efficiency) was found to be maximum and hence the variable X_1 for particle size and variable X_2 for entrapment efficiency were considered to be a major contributing variables of PLGA-TMZ-NP.

Contours

By keeping the major contributing independent variable fixed at -1, 0, +1 the contours were constructed between the other independent variables for particle size and drug entrapment efficiency separately.

For Etoposide, two dimensional contour plots for particle size and drug entrapment efficiency, from the reduced model based on equation 6 and equation 7, are shown in figures 4.2a, 4.2b, 4.2c and figures 4.3a, 4.3b, 4.3c respectively. The independent variable with highest coefficient was X_1 (polymer concentration) for both particle size and drug entrapment efficiency

Similarly, two dimensional contour plots for particle size and drug entrapment efficiency, from the reduced model based on equation 8 and equation 9, are shown in figures 4.4a, 4.4b, 4.4c and figures 4.5a, 4.5b, 4.5c respectively. The independent variable with highest coefficient was X_1 (polymer concentration) for both particle size and X_2 (%w/v PVA concentration) for drug entrapment efficiency

Check Point Analysis

For etoposide, at fixed levels of -1, 0 and 1 of independent variable X_1, three check points were selected one each on three plotted contours. Nanoparticles at these three checkpoints were prepared experimentally using the same procedure keeping the other process variables as constant, with the amounts of X_2 and X_3 at the selected check points. The computed values from the contours at -1, 0 and 1 level and the experimentally determined values for particle size and drug entrapment efficiency values are shown in Table 4.10. Both experimentally obtained and theoretically computed particle size and entrapment efficiency values were compared using student 't' test and the difference was found to be non significant ($p>0.05$; $p= 0.717$ for particle size and 0.629 for drug entrapment efficiency).

Similarly for temozolomide, the check point batches were selected from contours plotted at fixed levels of -1, 0 and 1 of independent variable X_1 (for particle size) and X_2 (for entrapment efficiency). The computed values from contours and the experimental values are recorded in Table 4.11 for particle size and Table 4.12 for drug entrapment efficiency. ($p=0.6008$ for particle size and $p=0.4483$ for drug entrapment efficiency).

This proves the role of a derived reduced polynomial equation and contour plots in the preparation of nanoparticles of etoposide and temozolomide of predetermined particle size and drug entrapment efficiency within the selected range of the independent variables.

Optimized batches

For Etoposide, the batch with particle size of 144 ± 7nm and drug entrapment efficiency of 65.4 ± 2.2 % prepared at 0 level of X_1 (50mg polymer 5mg drug), 0 level of X_2 (1%w/v PVA

in aqueous solution) and +1 level of X_3 (organic: aqueous phase of 1:2, i.e5ml of organic phase and 10ml of aqueous phase)was considered optimum based on the criteria of particle size <150nm with highest drug entrapment efficiency. Hence, 5mg of drug and 50mg of PLGA was dissolved in 5ml of (acetone: ethanol 90:10) and this solution was added to 10ml of 1%w/v PVA aqueous solution under constant moderate stirring.

Similarly for temzolomide, the batch with 132 ± 4nm particle size and 33.5 ± 1.1 % drug entrapment efficiency was considered to be optimum at the at 0 level of X_1 (50mg polymer 5mg drug), 0 level of X_2 (1%w/v PVA in aqueous solution) and +1 level of X_3 (organic: aqueous phase of 1:2, i.e5ml of organic phase and 10ml of aqueous phase).

The optimized batch for Temozolomide was prepared by saturating the aqueous phase with Temozolomide before addition of the organic phase. By pre-saturation of the aqueous phase with Temozolomide the drug entrapment efficiency was enhanced to 70.3 ± 2.4 % with no change in particle size. Hence, 5mg of drug and 50mg of PLGA was dissolved in 5ml of (acetone: ethanol 90:10) and this solution was added to 10ml of 1%w/v PVA aqueous solution pre saturated with Temozolomide under constant moderate stirring.

4.3.2 Lyophilization and optimization of cryoprotectant concentration

Freeze-drying has been the most utilized drying method of nanoparticle suspensions. Because the freeze-drying process is highly stressful for nanoparticles, addition of cryoprotectants becomes essential. For nanoparticles carbohydrates have been perceived to be suitable freeze-drying protectants. There are considerable differences in the cryoprotective abilities of different carbohydrates.

The optimized batch of nanoparticles was lyophilized using sucrose, mannitol and trehalose (at 1:1, 1:2 and 1:3 nanoparticle: cryoprotectant) to select suitable cryoprotectant and its concentration. The redispersibility of the freeze-dried formulations and particle size of the nanoparticles before and after freeze-drying were evaluated and recorded in table 4.13.

Table 4.13: Effect of different cryoprotectants on the particle size and redispersion

Type of cryoprotectant	NP: CP	Particle size (nm)		S_f/S_i	Redispersion
		Before lyophilization S_i	After lyophilization S_f		
Initial	1:0	144 ± 6	NA	NA	NA
Sucrose	1: 1	--	--	--	Poor redispersibility
Sucrose	1:2	--	528 ± 15	3.67	Poor redispersibility
Sucrose	1:3	--	410 ± 17	2.85	Poor redispersibility
Mannitol	1: 1	--	429 ± 15	2.98	Difficult redispersibility
Mannitol	1:2	--	358 ±14	2.49	Difficult redispersibility
Mannitol	1:3	--	310 ± 16	2.15	Difficult redispersibility
Trehalose	1: 1	--	234 ± 13	1.63	Easy redispersibility
Trehalose	1:2	--	182 ± 16	1.26	Easy redispersibility
Trehalose	1:3	--	149 ± 8	1.06	Easy redispersibility

(Mean ± S.D., $n = 3$)
NA: Not Applicable

With use of sucrose as the cryoprotectant, the cake formed after lyophilization was condensed and had collapsed structure. The redispersibility of nanoparticles with sucrose was poor and was only possible after sonication. At lowest ratio of 1:1, the lyophilized nanoparticles could not be redispersed completely. For the ratios of 1:2 and 1:3 particle size of the nanoparticles, as shown in table 4.13, increased significantly after lyophilization. The S_f/S_i values were 3.67, 2.85 with 1:2, 1:3 NPs: sucrose respectively. The increase in the particle size could have been due to the cohesive nature of the sucrose. Further, it was observed that the lyophilized nanoparticles with sucrose had tendency to absorb moisture very quickly.

With mannitol, the lyophilized nanoparticle product formed was fluffy and snow like voluminous cake. With mannitol, the nanoparticle formulation showed free flowing ability, however the redispersion was difficult and possible only after vigorous shaking. The particle size, recorded in table 4.13, after lyophilization increased significantly than the initial. The S_f/S_i values were 2.98, 2.49 and 2.19 with 1:1, 1:2 and 1:3 NPs: mannitol respectively. This may be due to the low solubility of mannitol in water i.e. 0.18 part of mannitol soluble in 1 parts of water.

With trehalose also, the lyophilized nanoparticles formed fluffy and snow like voluminous cake. With trehalose as cryoprotectant, the lyophilized nanoparticles were redispersed easily and the increase in particle size was not significant as indicated by S_f/S_i values which were 1.63, 1.26, and 1.04 for 1:1, 1:2 and 1:3 NPs: trehalose respectively recorded in table 4.13. The redispersion of the nanoparticles depends on the hydrophilicity of the surface. The easy redispersibility is probably due to the higher solubility of trehalose in water i.e. 0.7 parts in 1 part of water. The cryoprotective effect may be attributed to the ability of trehalose to form a glassy amorphous matrix around the particles, preventing the particles from sticking together during removal of water (Konan et al 2002). Also the very property of the tyndall effect observed with nanoparticles was retained after redispersion of the nanoparticles lyophilized using trehalose. Furthermore, trehalose, a non-reducing disaccharide of glucose, has previously exhibited satisfactory cryoprotective effects for pharmaceutical and biological materials (De Jaeghere et al 1999).

Therefore, trehalose at a ratio of 1: 3 (nanoparticles: trehalose) was used as cryoprotectant for lyophilization of optimized batch of nanoparticles for further studies.

4.3.3 Transferrin conjugation of nanoparticles

The scheme of Tf conjugation to the nanoparticles is shown in figure 4.6. The surface modification of PLGA-NPs with Tf was achieved in two steps involving the activation of the nanoparticles in the presence of catalyst zinc tetrafluoroborohydrate $[Zn(BF_4)_2]$ with epoxy compound (SR-4GL, hexa epoxy) which acts as linker, followed by attachment of transferrin to the nanoparticle at the other end of the epoxy compound. (Sahoo et al, 2004, Sahoo and Labhsetwar, 2005) It is reported that PVA cross links with PLGA surface in the form of residual PVA. (Sahoo et al 2002). As represented in the figure 4.6, atleast one of the epoxy of SR-4GL would have conjugated to the hydroxyl group of PVA and the other epoxy groups to the amine group of Tf. The amounts of activating agents SR-4GL and Tf were optimized to achieve minimum increase in particle size and maximum Tf density on the surface of NPs.

As reported by Sahoo and Labhsetwar, the amount of the catalyst was kept at 5mg during the entire conjugation study. The influence of the amount of epoxy compound on the density of surface Tf and particle size was evaluated keeping the amount of nanoparticles and the amount of Tf constant at 20mg and 10mg respectively and the results recorded in table 4.14 and graphically shown in figure 4.7 to 4.10.

Table 4.14: Influence of Concentration of Activating Agent

Activating agent SR-4GL (Epoxy compound)	Tf density (µg/mg)		Particle size (nm)	
	PLGA-ETP-NP	PLGA-TMZ-NP	PLGA-ETP-NP	PLGA-TMZ-NP
5	21.7±2.6	19.6±1.8	154.5±7.2	142±10
10	38.1 ± 3.4	32 ± 2.7	162.1±12	153.8±14
20	40.7±1.7	34.3±2.4	194±14.2	186±12.7

(Mean ± S.D., n = 3)

Figure 4.7: Influence of the concentration of the activating agent SR-4GL on Tf density at the surface of PLGA-ETP-NP

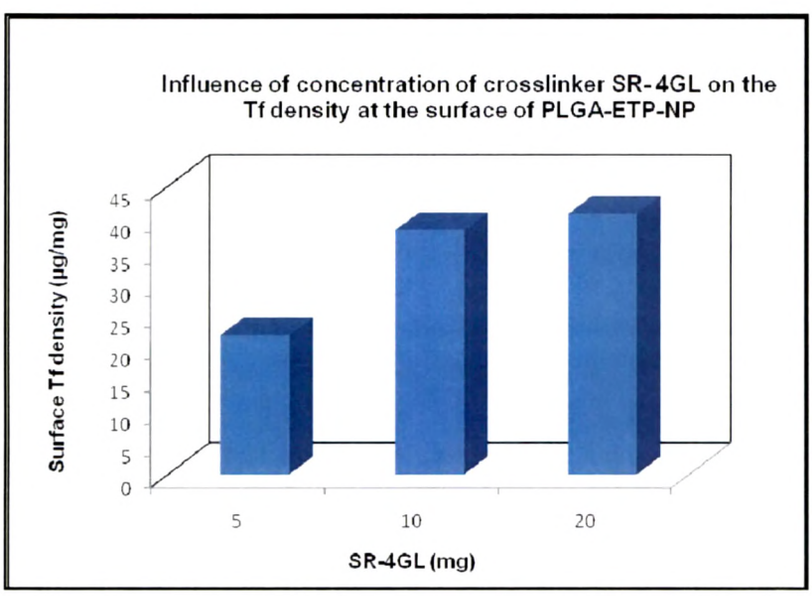

Figure 4.8: Influence of the concentration of the SR-4GL on the particle size of PLGA-ETP-NP

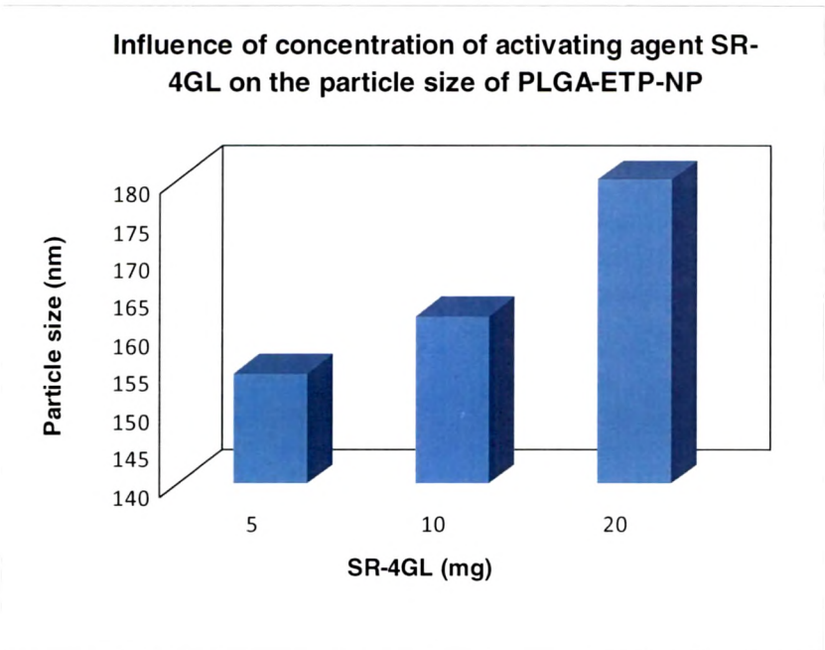

Figure 4.9: Influence of the concentration of the activating agent SR-4GL on Tf density at the surface of PLGA-TMZ-NP

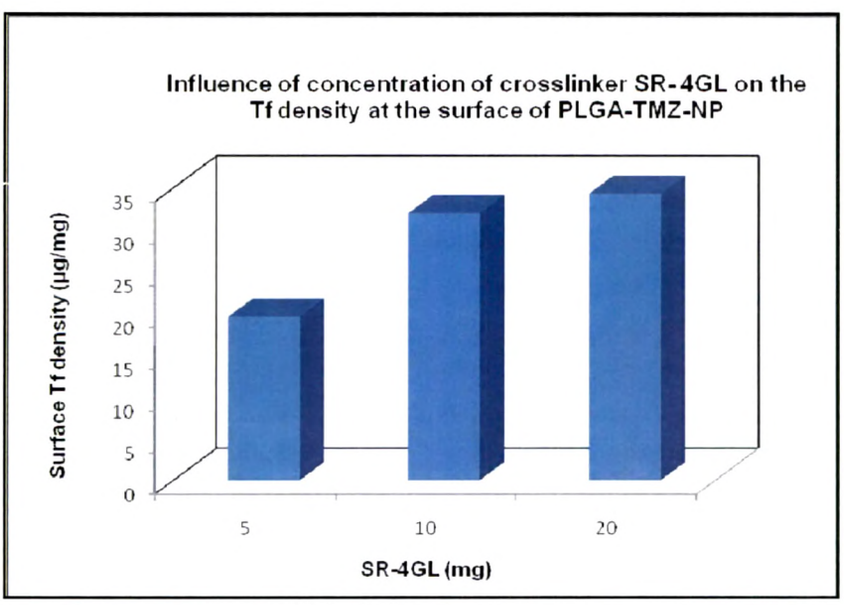

Figure 4.10: Influence of the concentration of the activating agent SR-4GL on the particle size of PLGA-TMZ-NP

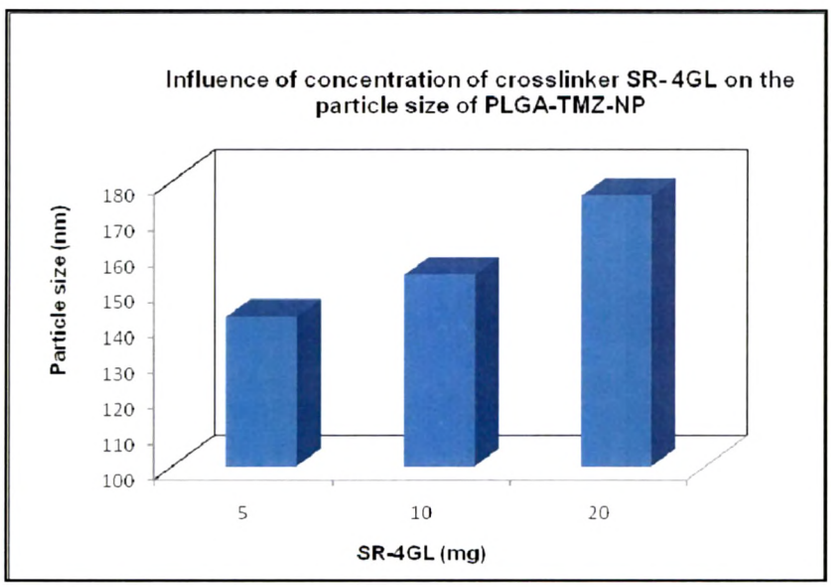

The amount of epoxy compound was varied at 5mg, 10mg and 20mg. With the increase in the amount of the epoxy from 5 to 10mg, the surface Tf density for Tf-PLGA-ETP-NP increased from 21.7µg/mg to 38.1µg/mg and the particle size increased from 154.5 nm to 162.1nm. Increasing further the epoxy compound to 20mg did not considerably increase the surface Tf density. However, the particle size increased from 162.1nm to 194 nm. Similar results were observed with Temozolomide nanoparticles. For TMZ the epoxy compound amount at 5, 10 and 20mg resulted in the surface Tf density of 19.6µg/mg, 32µg/mg and 34.3µg/mg respectively, with corresponding particle size of 142nm, 153.8nm and 186nm. The increase in the surface Tf density may be due to the increase in the number of the epoxy molecules reacting with hydroxyl of PVA and thereby increase in the availability of the epoxy groups for conjugation of Tf. The association of epoxy and Tf with nanoparticle is believed to have resulted in the increase in the particle size. Increasing the epoxy amount from 10mg to 20mg resulted in much increase in the particle size but the amount of the

transferrin conjugated did not increase significantly. Hence, the epoxy amount was optimized at 10mg for both Etoposide and Temozolomide nanoparticles.

To study the influence of Tf added on the surface Tf density and particle size, different amount of Tf in solution were added to 20mg activated PLGA-ETP-NP and PLGA-TMZ-NP. The measured surface Tf density and particle size are recorded in Table 4.15 and shown graphically in figure 4.11 to 4.14.

Table 4.15: Influence of amount of Transferrin

Amt of Tf added (mg)	Transferrin Density (µg/mg)		Particle size (nm)	
	PLGA-ETP-NP	PLGA-TMZ-NP	PLGA-ETP-NP	PLGA-TMZ-NP
2.5	16.1 ± 1.2	12.6 ± 1.4	151±6	140.2 ± 4
5	24.9±1.9	19.4 ± 2.8	154.7±9.9	148 ± 8.2
10	38.1±3.1	32 ± 2.64	162.1±12	153.8±14
20	46.4 ± 4.7	43.7±2.1	312±16.4	290±11

(Mean ± S.D., $n = 3$)

Figure 4.11: Influence of amount of Transferrin taken for conjugation on surface Tf density (µg/mg) of PLGA-ETP-NP

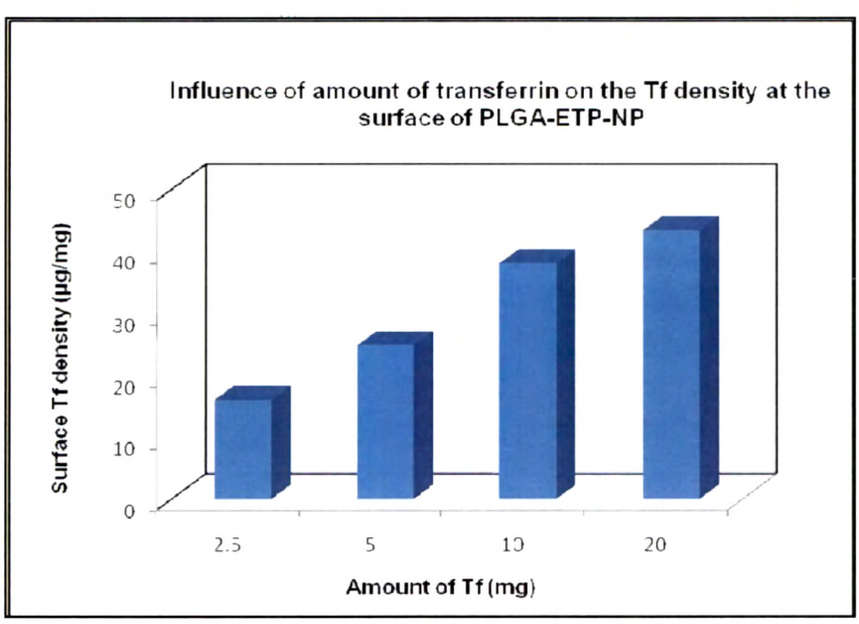

Figure 4.12: Influence of amount of Transferrin taken for conjugation on particle size of PLGA-ETP-NP

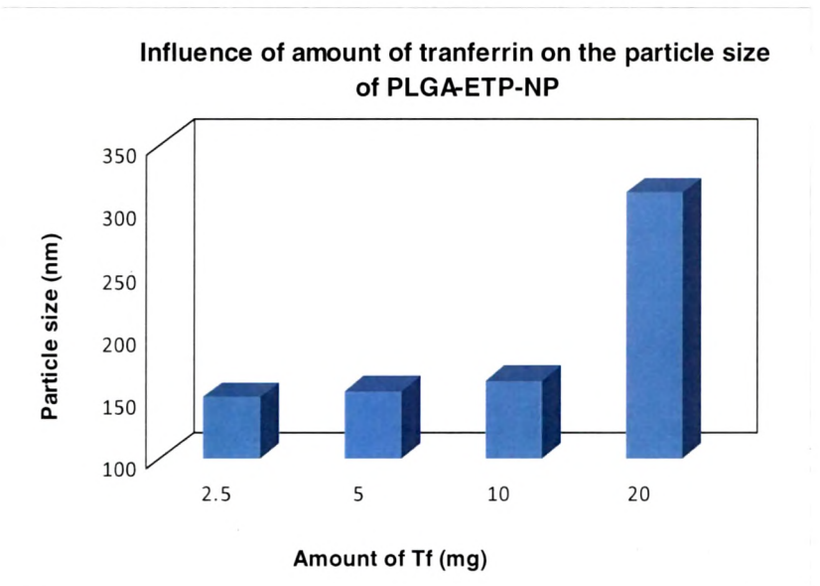

Figure 4.13: Influence of amount of Transferrin taken for conjugation on surface Tf density (µg/mg) of PLGA-TMZ-NP

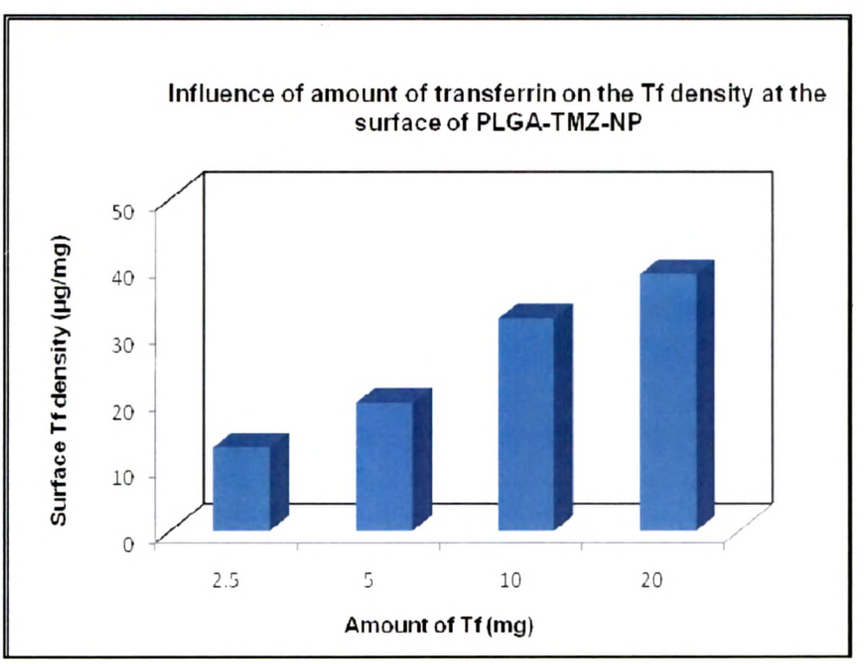

Figure 4.14: Influence of amount of Transferrin taken for conjugation on particle size of PLGA-TMZ-NP

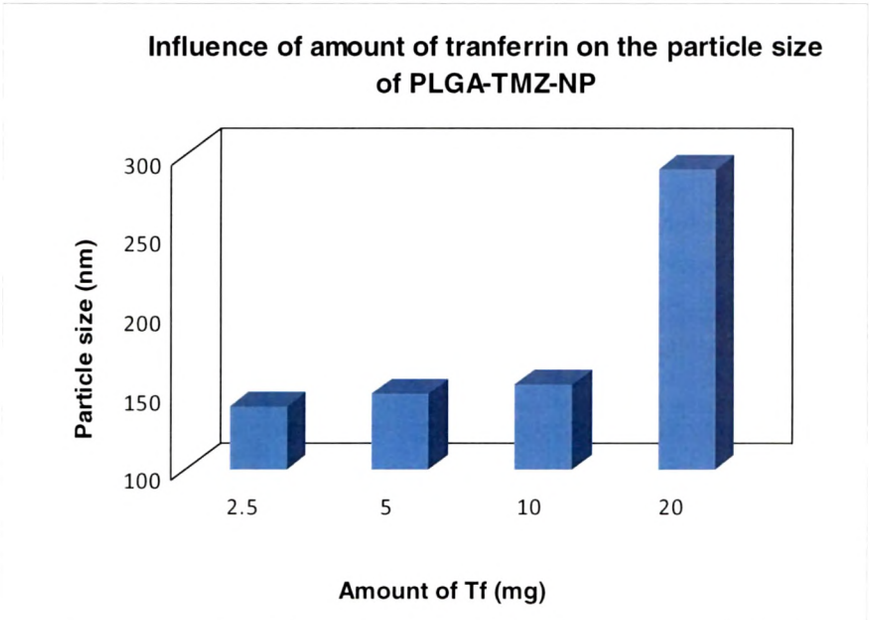

The amount of Tf was varied from 2.5mg to 20mg. For PLGA-ETP-NP, with increase in the amount of Tf from 2.5 to 10mg, the surface Tf density increased from 16.1µg/mg to 38.1µg/mg and the particle size increased from 151nm to 162.1nm. Further increasing the amount of Tf from 10mg to 20mg, the Tf density increased from 38.1µg/mg to 46.4 µg/mg. But the particle size increased from 162.1 to 312nm. Similarly for PLGA-TMZ-NP the surface Tf density and particle size were found to increase from 12.6µg/mg to 43.7µg/mg and 140nm to 290nm. With increase in the amount of Tf added for conjugation, the increase in the surface Tf density could have been due to the increase in the Tf molecule density available for conjugation. The increase in the particle size could have been due to increased surface Tf density. At the highest amount of Tf added for conjugation i.e 20mg, the particle size increased near to 300nm, probably due to the cross linking of Tf molecule with the epoxy groups of the neighboring molecules. For, intravenous administration, the preferable particle size is below 200nm and hence the 10mg Tf was considered as optimized amount.

The conjugation amino of Tf with the methylene of epoxy compound was confirmed by ^{1}H-NMR. Fig. 4.15 and Fig. 4.16 represent the ^{1}H-NMR of PLGA-ETP-NP and PLGA-TMZ-NP. The peaks at 2.36 and 2.39ppm represent the conjugation of amino group of Tf to the methylene group of epoxy compound.

Figure 4.15: ^{1}H-NMR of Tf -PLGA-ETP-NP

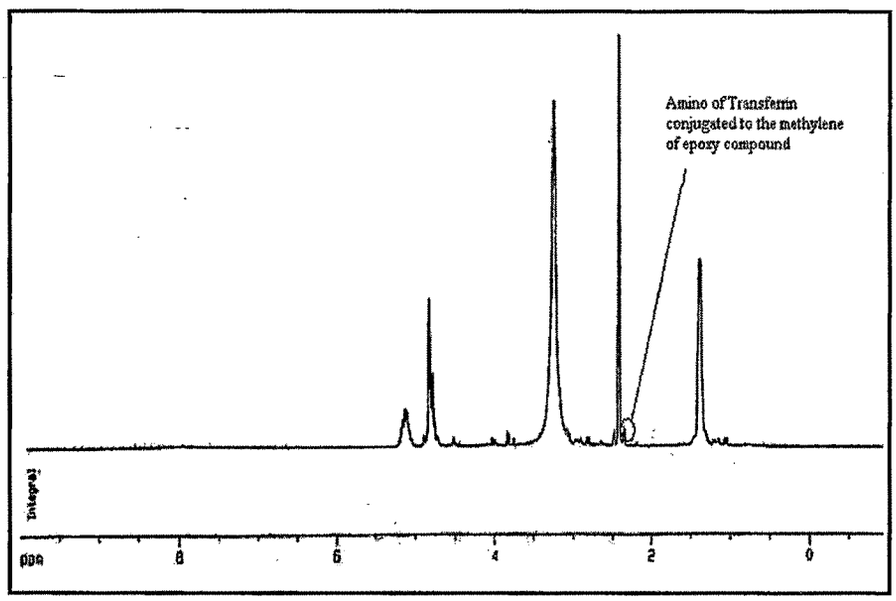

Figure 4.16: ^{1}H-NMR of Tf -PLGA-TMZ-NP

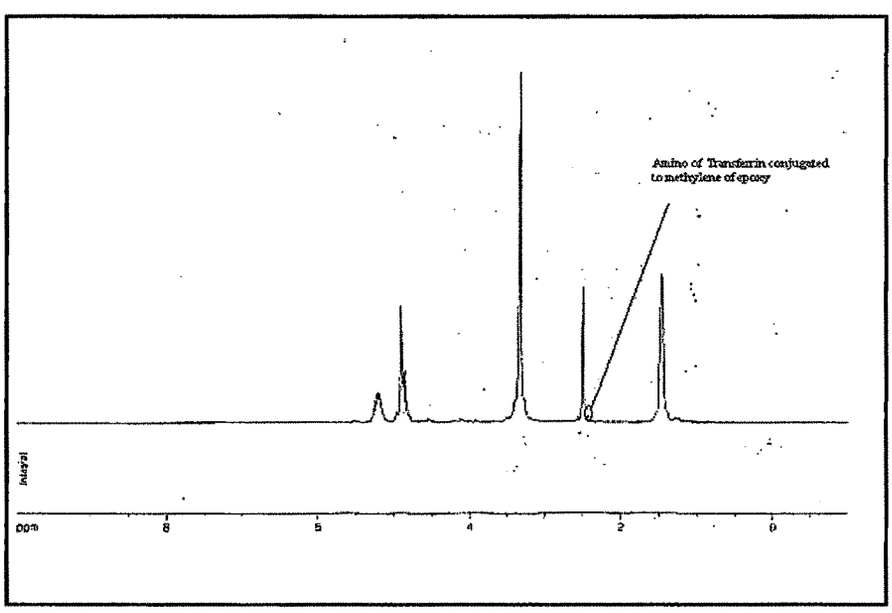

For further studies, Etoposide and Temozolomide nanoparticles were prepared using 5mg drug, 50mg PLGA, 10ml of 1%w/v PVA concentration in aqueous phase and organic: aqueous phase ratio of 0.5 (5ml of organic phase for 10ml of aqueous phase). For Temozolomide nanoparticles, the aqueous phase containing PVA was saturated with Temozolomide before addition of organic phase to aqueous phase. The nanoparticles were lyophilized using trehalose as cryoprotectant at 1:3 (nanoparticle: trehalose) ratio. The optimized nanoparticles were conjugated with transferrin using 10mg epoxy activating agent and 10mg transferrin for 20mg of nanoparticles. The unconjugated and conjugated nanoparticles of Etoposide and Temozolomide were characterized and subjected to stability studies.

4.4 Conclusions

PLGA Nanoparticles of etoposide and temozolomide were successfully prepared by nanoprecipitation method. The nanoparticles were surface conjugated with transferrin for preferential brain delivery. The particle observed for both unconjugated and transferrin conjugated nanoparticles was below 200nm suitable for intravenous administration.

References

- Anjali Sharma, Sadhna Sharma and G. K. Khuller. Lectin-functionalized poly (lactide-co-glycolide) nanoparticles as oral/aerosolized antitubercular drug carriers for treatment of tuberculosis. Journal of Antimicrobial Chemotherapy (2004) 54, 761–766

- Barbara Stella, Silvia Arpicco, Maria Teresa Peracchia, Didier Desmaële, Johan Hoebeke, Michel Renoir, Jean D'Angelo, Luigi Cattel, Patrick Couvreur Design of folic-acid-conjugated nanoparticles for drug delivery. Journal of Pharmaceutical Sciences. 89 (11) (2000) 1452-1464

- Chorny M., Ilia Fishbein, Haim D. Danenberg , Gershon Golomb. L ipophilic drug loaded nanospheres prepared by nanoprecipitation: effect of formulation variables on size, drug recovery and release kinetics. Journal of Controlled Release 83 (2002) 389–400

- De Jaeghere, F., Alle′ mann, E., Leroux, J. C., Stevels,W., Feijen, J., Doelker, E., Gurny, R. (1999) Formulation and lyoprotection of poly (lactic acid-co-ethylene oxide) nanoparticles: influence on physical stability and in vitro cell uptake. Pharm. Res. 16: 859–866

- Derakhshandeh K., M. Erfan., S. Dadashzadeh. Encapsulation of 9-nitrocamptothecin, a novel anticancer drug, in biodegradable nanoparticles: Factorial design, characterization and release kinetics. European Journal of Pharmaceutics and Biopharmaceutics 66 (2007) 34–41

- Fessi, H., Puisieux, F., Devissaguet, J. P., Ammoury, N., and Benita, S. 1989. Nanocapsule formation by interfacial polymer deposition following solvent displacement. *Int. J. Pharm.* 55:R1-R4.

- Guerrero D. Q., E. Allemann, H. Fessi, E. Doelker, Preparation techniques and mechanisms of formation of biodegradable nanoparticles from performed polymers, Drug Dev. Ind. Pharm. 24 (12) (1998) 1113–1128

- Haley, E. Frenkel, Nanoparticles for drug delivery in cancer treatment, Urol. Oncol. 26 (1) (2008) 57–64.

- J.D. Byrne et al. / Advanced Drug Delivery Reviews 60 (2008) 1615–1626

- Konan YN, Gurny R, Konan YN, Gurny R, et al. Preparation and characterization of sterile and freeze-dried sub-200nm nanoparticles. Int J Pharm 2002; 233:239–52

- Levison KK, Takayama K, Isowa K, Okaba K, Nagai T. Formulation optimization of indomethacin gels containing a combination of three kinds of cyclic monoterpenes as percutaneous penetration enhancers. *J Pharm Sci.* 1994;83:1367-1372.

- Misra A., Sheth A. K., 2002. Mathematical modeling of preparation of acyclovir liposomes:reverse phase evaporation method, J Pharm Pharmaceut Sci, 5(3), 285-291

- P.D. Scholes, A.G.A. Coombes, L. Illum *et al.*, The preparation of sub-200 nm poly (lactide-co-glycolide) microspheres for site-specific drug delivery. *J. Controlled Release* **25** (1993), pp. 145–153.

- Panyam, J.; Sahoo, S. K.; Prabha, S.; Bargar, T.; Labhasetwar, V. Fluorescence and electron microscopy probes for cellular and tissue uptake of poly(D,L-lactide-co-glycolide) nanoparticles. Int. J. Pharm. 2003, 262, 1-11.

- R. Langer, Tissue engineering: a new field and its challenges. Pharm. Res. **14** 7 (1997), pp. 840–841.

- R.A. Jain , The manufacturing techniques of various drug loaded biodegradable poly(lactide-co-glycolide) devices. Biomaterials **21** (2000), pp. 2475–2490.

- S.K. Sahoo et al. / Journal of Controlled Release 82 (2002) 105 –114

- S.M. Moghimi, A.C. Hunter and J.C. Murray, Long-circulating and target specific nanoparticles: theory to practice. Pharmacol. Rev. **53** 2 (2001), pp. 283–318.

- Saez, M. Guzman, J. Molpeceres, and M.R. Aberturas, Eur. J. Pharm.Biopharm. 50, 379 (2000)

- Sanjeeb K. Sahoo, Wenxue MA1 and Vinod Labhasetwar Efficacy of transferrin-conjugated paclitaxel-loaded Nanoparticles in a murine model of prostate cancer Int. J. Cancer: 112, 335–340 (2004)

- Sahoo, S.K. and Labhasetwar, V., 2005. Enhanced Antiproliferative Activity of Transferrin-Conjugated Paclitaxel-Loaded Nanoparticles Is Mediated via Sustained Intracellular Drug Retention Molecular Pharmaceutics, Vol. 2, No. 5, 373-383

- Shirakura O, Yamada M, Hashimoto M, Ishimaru S, Takayama K, Nagai T. Particle size design using computer optimization technique. Drug Dev Ind Pharm. 1991;17:471-483.

- Si Shen Feng, Nanoparticles of biodegradable polymers for new-concept chemotherapy, Expert Reviews Medical Devices 1 (1), 115-125, 2004

- Song X, Yu Zhao, Wenbin Wu, Yueqi Bi, Zheng Cai, Qiuhong Chen, Yuanbo Li, Shixiang Hou. PLGA nanoparticles simultaneously loaded with vincristine sulfate and verapamil hydrochloride: Systematic study of particle size and drug entrapment efficiency. International Journal of Pharmaceutics 350 (2008b) 320–329.

- Song Xiangrong, Yu Zhao, Shixxiang Hou, Fangyuan Xu, Rongli Zhao, Junyao He, Zheng Cai, yuano Li, Qiuhong Chen. Dual agents loaded PLGA nanoparticles: systematic study of particle size and drug entrapment efficiency. European Journal of pharmaceutics and biopharmaceutics 69 (2008a) 445-453.

- T. Minko, Advanced Drug. Deliv. Rev. 56-491 (2004)

- V. Labhasetwar ,-Nanoparticles for drug delivery. Pharm. News **4** (1997), pp. 28–31.

- Vandervoort J., S. Bozdag, K. Dillen, and A. Ludwig, The effect of freeze-drying with different cryoprotectants and gamma-irradiation sterilization on the characteristics of ciprofloxacin HCl-loaded poly(D,L-lactide-glycolide) nanoparticles , Journal of Pharmacy and Pharmacology, 2005, 57, 699-707